Synthesis, characterization and antimicrobial activity of some new azo dyes derived from 4-hydroxy-6-methyl-2H-pyran-2-one and its dihydro derivative

Franck Le Bideau, Soumaya Ben Mohamed-Smati, Fadhil Lafta Faraj, Imène Becheker, Hadjira Berredjem, Maamar Hamdi, Françoise Dumas, Yahia Rachedi

Synthesis, characterization and antimicrobial activity of some new azo dyes derived from 4-hydroxy-6-methyl-2H-pyran-2-one and its dihydro derivative

Soumaya Ben Mohamed-Smati,[a] Fadhil Lafta Faraj,[a] Imène Becheker,[b] Hadjira Berredjem,[b] Franck Le Bideau,[c] Maamar Hamdi,[a] Françoise Dumas*[c] and Yahia Rachedi*[a]

[a] Laboratory of Applied Organic Chemistry, Faculty of Chemistry, University of Science and Technology Houari Boumediene, BP 32, El-Alia, 16111, Bab-Ezzouar, Algiers, Algeria. E-mail: yrachedi@usthb.dz

[b] Laboratory of Applied Biochemistry and Microbiology, Faculty of Sciences, Department of Biochemistry, University Badji Mokhtar, Annaba, Algeria

[c] Laboratory BioCIS, UMR CNRS 8076, CoSMIT, Université Paris Sud- CNRS, Université Paris Saclay, Faculté de Pharmacie, 5, rue Jean-Baptiste Clément, 92296 Châtenay-Malabry Cedex, France. E-mail: francoise.dumas@u-psud.fr

† Corresponding author

Abstract: A series of new azo disperse dyes was synthesized by coupling 4-hydroxy-6-methyl-2H-pyran-2-one (triacetic acid lactone, TAL) or its hydrogenated derivative 4-hydroxy-6-methyl-5,6-dihydro-2H-pyran-2-one (dihydro triacetic acid lactone, DHTAL) with diazonium salts derived from aniline, 4-bromoaniline, 4-nitroaniline, 4-methoxyaniline, 2,4-dimethoxyaniline and 2,5-dimethoxyaniline. Spectroscopic data of these dyes dissolved in five organic solvents were measured. The effects of solvent polarity, nucleophilic component and substituent nature on the visible absorption spectra of the dyes are also reported. The structures of all compounds were confirmed by FT-IR, electronic absorption in UV and visible regions, ^{1}H, ^{13}C and 2D NMR and high resolution mass spectroscopy (HRMS). In addition, *in vitro* antibacterial activity of the synthesized derivatives against Gram positive and Gram negative bacteria, both reference and clinical strains, was evaluated qualitatively and quantitatively by agar diffusion method.

Keywords: Azo dye, Pyran-2-one,Solvent effect, Substituent effect, Tautomerism, Antimicrobial activity

1. Introduction

Azo dyes are the oldest and the largest used class of industrially synthesized organic dyes due to their versatile application in various fields [1], such as dyeing textile, leather, paper, food and cosmetic products [2-4], and for biomedical studies and applications [5]. They are also used in high technology areas as laser [3-4], photodynamic therapy [6] and dye sensitized solar cells [7].

Azo compounds contain at least a conjugated azo chromophore, (-N=N-), linking two aromatic systems [8-13]. Generally, the synthesis of azo dyes involves two steps (Figure 1). The first one is the conversion of an aromatic amine to a diazo compound, a process known as diazotation, and the second step is the reaction of the titled diazo compound with a nucleophilic component to produce the corresponding azo dye, a process known as diazo

coupling. This process is suitable for forming both azo dyes and pigments [8,9]. Among them, the azo dyes derived from enol type coupling components constitute an interesting type of compounds since they potentially have several tautomeric forms (enol-azo, keto-azo, hydrazo) in solution and solid state [10,13-16]. Some important investigations have been carried out on the synthesis and spectroscopic behavior of heteroarylazo dyes based on 4-hydroxycoumarin [14-16], 4-hydroxyquinolone [13,17], 2-hydroxyacetophenone [11] and 4,6-dihydroxypyrimidine [18] as an enol type coupling component, as well as other heteroarylazo compounds [19-23].

In view of these encouraging reports, and in line with our interest to develop the chemistry of bio-based resources [24], in this study we report on the synthesis of two series of some new azo compounds and the investigation of their spectroscopic properties. In the first one, 4-hydroxy-6-methyl-2H-pyran-2-one (**1**) (triacetic acid lactone, TAL) and in the second series its hydrogenated derivative, 4-hydroxy-6-methyl-5,6-dihydro-2H-pyran-2-one (**2**) (dihydro triacetic acid lactone, DHTAL) were chosen as coupling components in reaction with some diazotized aromatic amines as diazo components (Figure 1). The structures of all products were confirmed by IR, UV–Vis, ^{1}H NMR, ^{13}C NMR, 2D-NMR and HRMS.

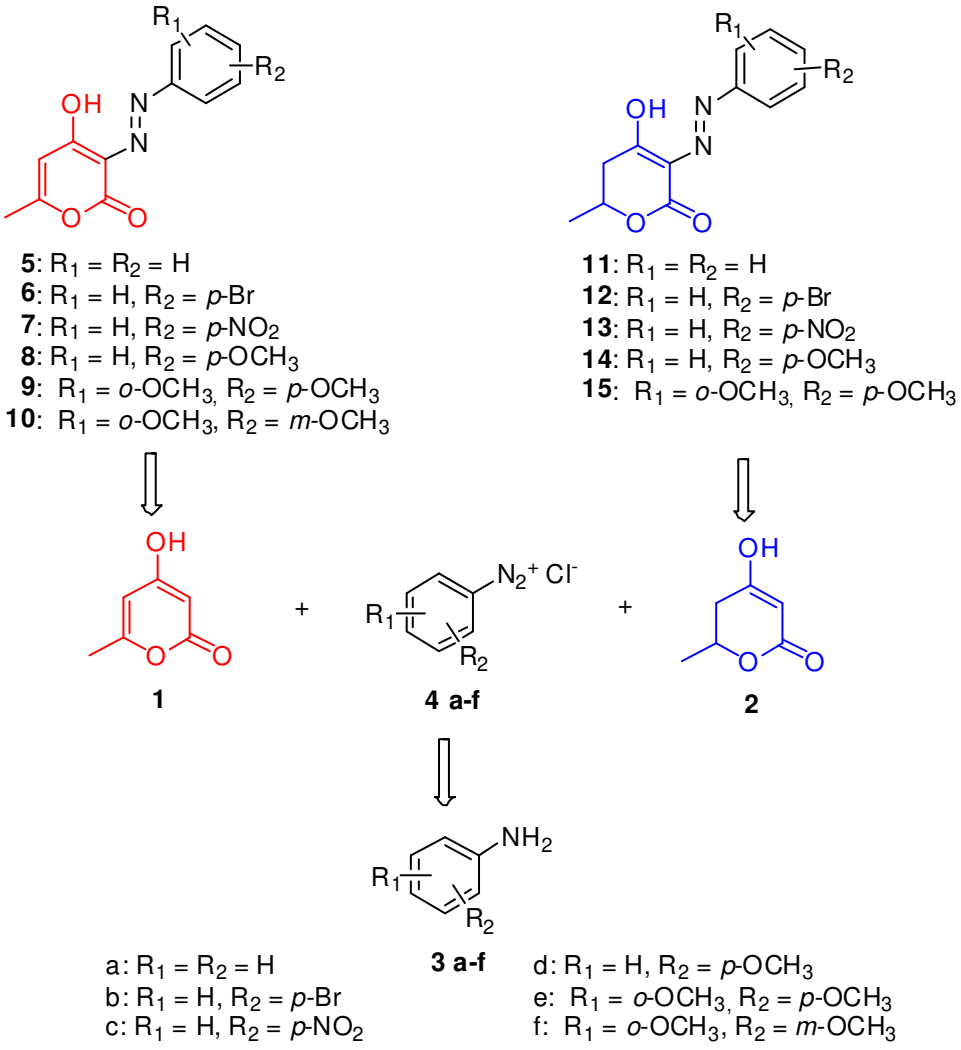

Fig. 1. Synthetic strategy to azo dye structures **5** – **15**.

Furthermore, infectious diseases caused by resistant microorganisms are responsible for increased health costs as well as high morbidity and mortality. Hence, there is an urgent need for discovery and development of novel antibiotics [25-28]. Therefore, the *in vitro* antimicrobial activity of all synthesized dyes against six bacterial strains, either reference or clinical, were examined in detail.

2. Results and Discussion

2.1. UV-Vis absorption spectra

*2.1.1. Effects of solvent polarity on photo physical properties of dyes **5** – **15***

The UV–Vis electronic spectra were recorded in the wavelength range 300 – 600 nm at concentration of approximately 10^{-5} to $2.5.10^{-5}$ mol.L^{-1} depending on the solubility of the dye,

the higher concentration corresponding to dye **11**. To assess the effect of solvent polarities on photophysical properties absorption of dyes, dyes **5** – **10** synthesized from TAL **1** as well as disperse dyes **11** – **15** synthesized from DHTAL **2** were analyzed in five different organic solvents having different polarity, dielectric constant (ε), and solvatochromic parameters (α, β, and π^* values) such as *n*-hexane, ethanol, acetone, acetonitrile and dichloromethane.

From the presented values in table 1, it is apparent that practically no solvatochromism was observed. The electronic absorption spectra showed absorption maxima in the region at 400 – 447 nm and 375 – 422 nm in n-hexane, 401 – 458 nm and 377 – 429 nm in acetone, 401 – 458 nm and 379 – 430 nm in acetonitrile, 417 – 463 nm and 387 – 436 nm in dichloromethane, 402 – 466 nm and 385 – 438 nm in ethanol for dyes **5** – **10** and **11** – **15**, respectively as illustrated for prototype compounds **5** (Figure 2a) and **11** (Figure 2b). In the UV–Vis spectra of these compounds (**5** – **15**) two absorptions are noteworthy in all tested solvents. The first one is a shoulder at 368 – 372 nm and the second one is a band between 400 – 466 nm for **5** – **10** and 375 – 438 nm for **11** – **15** (see Figure 2 for **5** and **11**).

Table 1

Influence of solvent on maximum wavelength of absorption (λ_{max}) of dyes **5** – **15**.

Structure	**Dye**	**λ_{max}** (nm)					**$\Delta(\lambda_{max})$** (nm)
		Hexane	Acetone	CH_3CN	CH_2Cl_2	EtOH	
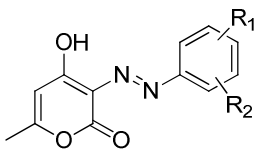	**5**	400.6	401.6	401.6	418.6	413.4	18
	6	423.2	418.4	415.8	424.4	421.2	8.6
5: $R_1 = R_2 = H$ **6:** $R_1 = H$, R_2 = p-Br **7:** $R_1 = H$, R_2 = p-NO_2 **8:** $R_1 = H$, $R_2 = p$-OCH_3 **9:** R1 = *o*-OMe, $R_2 = p$-OMe **10**: R1 = *o*-OMe, R2 = *m*-OMe	**7**	-	405.3	401.6	417.2	402.2	15.6
	8	428.4	437.8	436.4	443.8	442.4	15.4
	9	440.0	458.6	458.2	462.6	466.4	26.4
	10	447.0	454.8	453.8	461.0	442.4	18.6

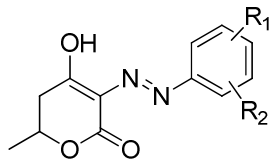

11: $R_1 = R_2 = H$
12: $R_1 = H$, $R_2 = p$-Br
13: $R_1 = H$, $R_2 = p$-NO_2
14: $R_1 = H$, $R_2 = p$-OMe
15: $R_1 = o$-OMe, $R_2 = p$-OMe

11	375.8	377.5	379.2	387.8	385.8	12.0
12	390.8	379.2	381.8	400.4	390.0	21.2
13	392.8	387.8	389.0	393.6	388.4	5.8
14	413.2	401.6	410.8	418.0	417.6	16.4
15	422.8	429.4	430.6	436.0	438.2	15.4

It can be suggested that dyes may exist as a mixture of two tautomeric forms which are in equilibrium. Furthermore, the spectra of unsubstituted derivatives **5** and **11** in various solvents showed small changes in their maximum absorption wavelength λ_{max} changing from 400 nm in *n*-hexane to 418 nm in dichloromethane and from 375 nm in *n*-hexane to 385 nm in EtOH, respectively (Table 1). This small variation, $\Delta(\lambda_{max})$ up to 26.4 nm (Table 1), suggests that the dyes are involved in strong intramolecular hydrogen bond.

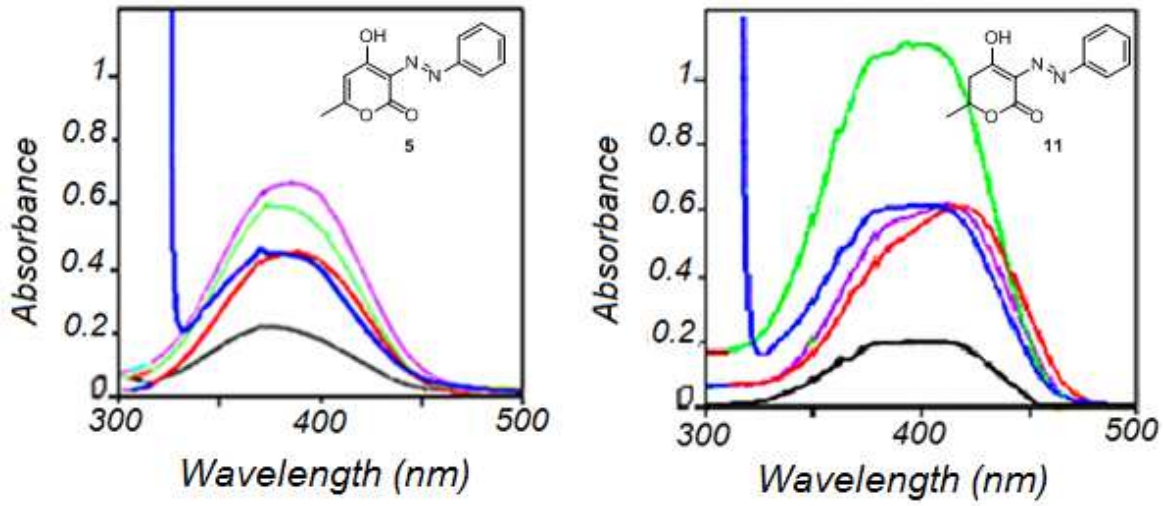

Fig.2 a. UV-vis absorption spectra of dye **5** (left) and **b.** dye **11** (right) in various solvents (black: n-hexane; red: dichloromethane; blue: acetone; violin: ethanol; green: acetonitrile).

2.1.2. Nucleophilic component effects

From typical spectroscopic data, a comparison of azo dyes **5** – **10** containing a 4-hydroxy-6-methyl-2H-pyran-2-one moiety with the parallel series of azo dyes **11** – **15** containing a hydrogenated derivative of 4-hydroxy-6-methyl-2H-pyran-2-one moiety revealed that dyes **5**

– **10** showed a red shift as compared to dyes **11** – **15** which showed a blue shift in all used solvents. For dye **5**, $\delta\lambda_{max}$ = 40 nm relative to dye **11** λ_{max} in dichloromethane (Table 1, Figure 3). For dye **6** $\delta\lambda_{max}$ = 39 nm relative to dye **12** λ_{max} in acetone (Table 1).

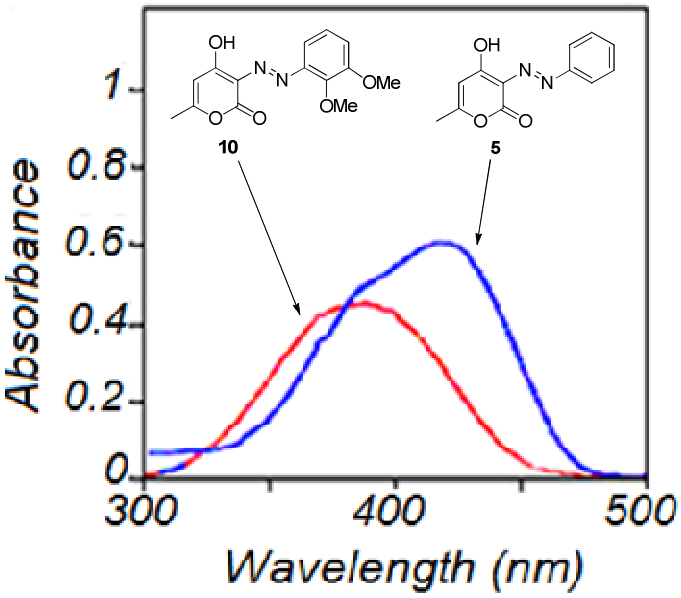

Fig. 3. UV-vis absorption spectra of dyes **5** (blue) and **11** (red) in dichloromethane.

2.1.3. Substituent effects

As is apparent in table 1, the introduction of electron-donating methoxy group into the benzene ring results in bathochromic shifts in all solvents with respect to unsubstituted and electron-withdrawing nitro substituted aryl groups. For instance, for dye **8**, $\delta\lambda_{max}$ = 30 nm relative to dye **5** and $\delta\lambda_{max}$ = 40 nm relative to dye **7** λ_{max} in ethanol (Figure 4). For dye **14**, $\delta\lambda_{max}$ = 32 nm relative to dye **11** λ_{max} and $\delta\lambda_{max}$ = 29 nm relative to dye **13** λ_{max} in ethanol. Similarly, the introduction of electron-donating *o,p*-dimethoxy group in the aryl ring increases bathochromic shift in all solvents with respect to electron-donating *p*-methoxy and *p*-bromo groups, electron-withdrawing nitro group and unsubstituted aryl. Thus in ethanol, $\delta\lambda_{max}$ = 24, 45, 54 and 64 nm for dye **9** relative to dyes **8**, **6**, **7** and **5** λ_{max}, respectively (Figure 4), while $\delta\lambda_{max}$ = 21, 48, 50 and 52 nm for dye **15** relative to dyes **14**, **12**, **13** and **11** λ_{max} respectively.

These results can be attributed to the electron withdrawing nature of the hydroxypyrane moiety of the dyes.

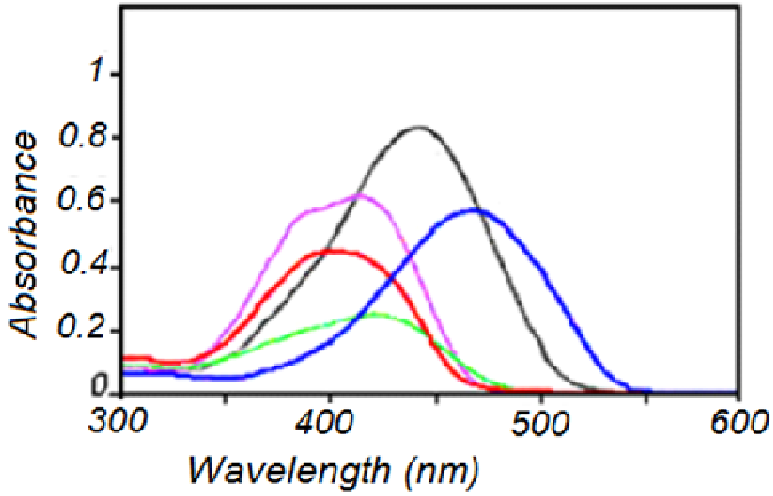

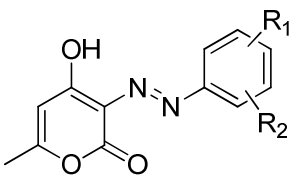

5: $R_1 = R_2 = H$
6: $R_1 = H$, $R_2 = p$-Br
7: $R_1 = H$, $R_2 = p$-NO_2
8: $R_1 = H$, $R_2 = p$-OCH_3
9: $R_1 = o$-OCH_3, $R_2 = p$-OCH_3
10: $R_1 = o$-OCH_3, $R_2 = m$-OCH_3

Fig. 4. Absorption spectra of dyes **5** (violin), **6** (green), **7** (red), **8** (black) and **9** (blue) in ethanol.

The azo-hydrazone tautomerism behavior of dyes formally derived from 1,3-dicarbonyl compounds is now well understood [29-32]. As shown in scheme 1, the synthesized azo dyes may exist in four possible tautomeric forms, tautomer **T1** named enol-azo-keto (EAK), two tautomers **T2** and **T3** as keto-hydrazo-keto (KHK1 and KHK2) forms, and **T4**, a keto-azo-enol (KAE) tautomer.

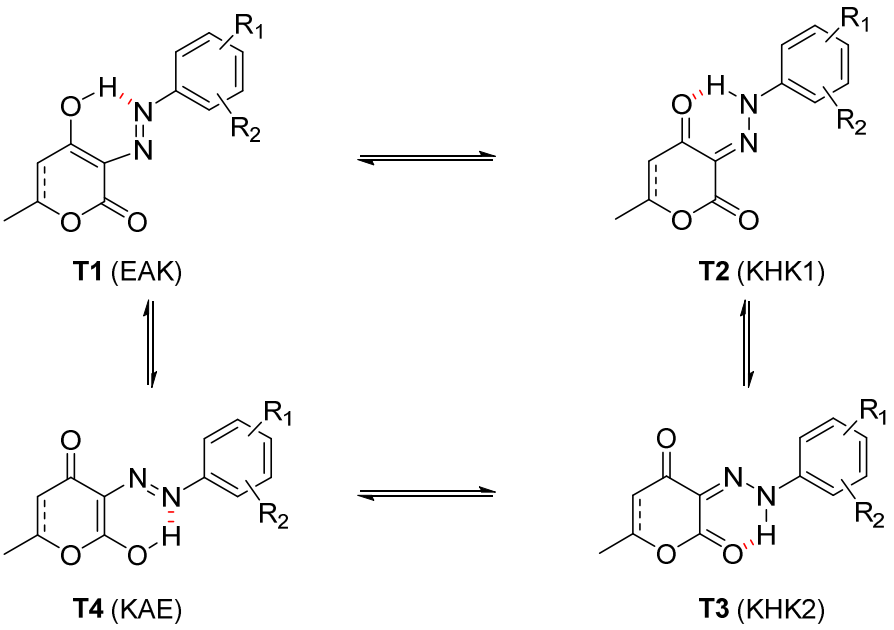

Scheme 1. Four possible tautomeric forms of the prepared azo dyes.

2.2. IR absorption spectra

The infrared spectra of dyes **5** – **10** and new dyes **11** – **15** were recorded in KBr disks and their characteristic IR absorption bands determined. The IR spectral data of the compounds studied indicate that they exist in the keto-hydrazo-keto (KHK1 and KHK2) forms **T2** and **T3** and in the enol-azo-keto (EAK) **T1** or keto-azo-enol (KAE) **T4** ones. Thus all compounds exhibit a weak and a broad NH stretching band in the region 3100 - 3000 cm^{-1}, the low frequency and the broadening of this group indicate that it is strongly involved in hydrogen bonding in the solid state. In the carbonyl region, each of the compounds studied exhibits two bands: the first one in the region 1600 – 1650 cm^{-1} and the second one in the region 1700 – 1750 cm^{-1} due to their stretching vibrations of the 4-carbonyl and α-pyrone groups, respectively. Such an assignment is substantiated by the IR spectra of azo dye monophenylhydrazones of 4-hydroxycoumarine **16** and *γ*-phenyl-*Δβ,γ*-butenolide **17** (Figure 5) which show their carbonyl stretching bands near 1620 and 1630 cm^{-1}, respectively [14]. The observed downward shift of the carbonyl stretching band in the compounds **5** – **10** and **11** – **15**, by analogy to 4-hydroxycoumarine and *γ*-phenyl-*Δβ,γ*-butenolide

monophenylhydrazones, is due to the conjugation with the C=N double bond as observed in the hydrazone tautomers **T2** and **T3** (KHK1 and KHK2) (Scheme 1). The IR spectra also showed bands in the region 2830 – 2970 cm^{-1} and 1500 – 1520 cm^{-1} which were assigned to aromatic C–H and C=N vibrations, respectively.

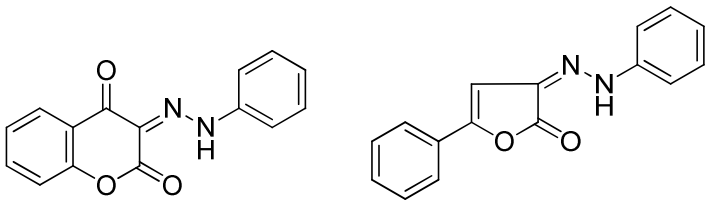

16 **17**

Fig. 5. Molecular structures of monophenylhydrazones of 4-hydroxycoumarine **16** and *γ*-phenyl-*Δβ,γ*-butenolide **17**.

2. 3. NMR and HRMS analysis

Furthermore, structure elucidations of these two series were confirmed by ^{1}H and ^{13}C NMR, 2D-NMR and HRMS data as described in detail for representative compounds **10** and **11**.

The ^{1}H NMR spectrum of compound **10** in $CDCl_3$ showed characteristic singlets for CH_3 and C5-proton of pyran ring at 2.23 and 5.83 ppm, respectively. The three aromatic protons appeared as one doublet of doublet centered at 6.82 ppm and two doublets centered at 6.90 and 7.50 ppm, respectively. The broad peaks at 14.37 ppm and 16.34 ppm were assigned to protons of the tautomeric hydrazone (=N–NH–) and hydroxyl (-O–H) motifs, respectively. These results confirm that dye **10** may exist as a mixture of keto-hydrazo-keto (KHK1 and KHK2) tautomers **T2** and **T3** and azo (EAK and KAE) tautomers **T1** and **T4** [30-32]. As shown by ^{1}H NMR spectra, dyes **5** – **9** may also exist as a mixture of keto-hydrazo-keto (KHK1 and KHK2) tautomers **T2** and **T3** in $CDCl_3$ solutions. The relative proportions of these sets of tautomers were determined by ^{1}H NMR spectroscopy of **5** – **10** by integration of the hydrazone proton signal (between 14.08 and 14.62 ppm in $CDCl_3$) relative to the corresponding enol proton signal (between 16.26 and 16.50 ppm in $CDCl_3$). These

proportions were in the range of 88% to 92% thus showing that azo tautomers **T1** and **T4** are predominant relative to hydrazo tautomers **T2** and **T3** in $CDCl_3$.

The ^{13}C NMR spectrum of compound **10** shows peaks at 20.6, 160.1 ppm for pyran methyl and carbonyl carbons respectively, and at 101.4, 115.7 and 144.2 ppm for aromatic carbons. Further support for the presence of azo motif (–N=N–) was provided by the signals at 125.5 and 130.3 ppm attributed to C_3 and C_8, respectively. From the HSQC spectrum, we conclude that protons resonance at σH 2.23, 3.83, 3.94, 5.83, 6.83, 6.91 and 7.50 ppm are bonded to the carbons appearing at σC 20.5, 56.2, 56.6, 107.8, 115.7, 112.7 and 101.4 ppm, respectively (Figure 6a). The HSQC spectrum allowed us to assign all protonated carbon resonances, while the connectivities from the HMBC spectrum (e.g. 3.83 → 154.9, 5.83 → 20.5, 122.5 and 166.1; 6.82 → 101.4 and 144.2; 7.50 → 115.7, 130.3, 144.2 and 154.9) (Figure 6b) support the structure of dye **10**. ESI-HRMS for this formula (M =$C_{14}H_{15}N_2O_5$) gave m/z (%) values at 291.0990 (100) and 313.0806 (72) attributed to the cations $[M+H]^+$ and $[M+Na]^+$, respectively. All together, these spectroscopic data are clearly consistent with the formation of the target product **10**.

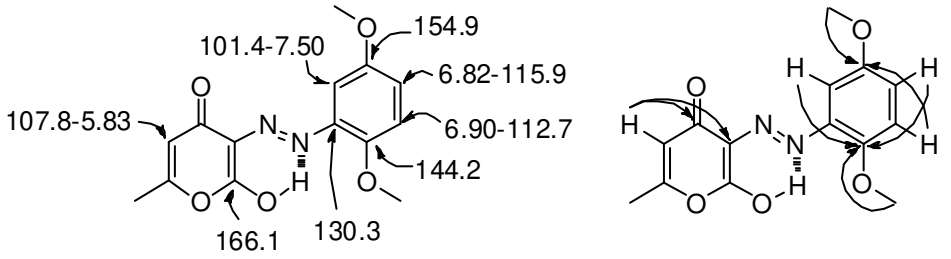

Fig. 6 a. Selected ^1H and ^{13}C NMR chemical shifts (right), **b.** HMBC correlations (left) of compound **10**.

The structure of the second series of new dyes was also confirmed on the basis of HRMS and NMR data. Interestingly, the molecular ion peak of compound **11** was found in the mass spectrum at *m/z* (%) 233.0921 (100) corresponding to $[M+H]^+$ of molecular formula $C_{12}H_{13}N_2O_3$. ^1H NMR spectroscopic analysis of **11** confirms the presence of both

hydrogenated pyran ring and aromatic nucleus. The spectrum showed a triplet centered at 1.53 ppm, two multiplets at 2.71 – 2.89 ppm and 4.68 – 4.83 ppm which belong to hydrogenated pyran protons. The aromatic protons resonated as three multiplets at 7.24 – 7.31 ppm, 7.41 – 7.46 ppm and 7.52 – 7.58 ppm. The broad peaks at 13.88 ppm and 15.16 ppm were respectively assigned to the hydrazone (=N–NH–) and enol (=C–OH) protons of the tautomers. In the ^{13}C NMR spectra and from the HMBC charts of azo compound **11**, it was concluded that the peaks resonating at σC =21.2, 44.9 and 192.2 ppm correspond to methyl C_7, methine C_5 and carbonyl C_4 carbon atoms of hydrogenated pyran, respectively, whereas the phenolic carbon atoms appeared at σC =117.7 and 130.1 ppm. The signals at σC =122.9 and 141.1 ppm were attributed to C_3 and C_8 respectively which confirmed the presence of the hydrazone motif (=N–NH–) (Figure 7).

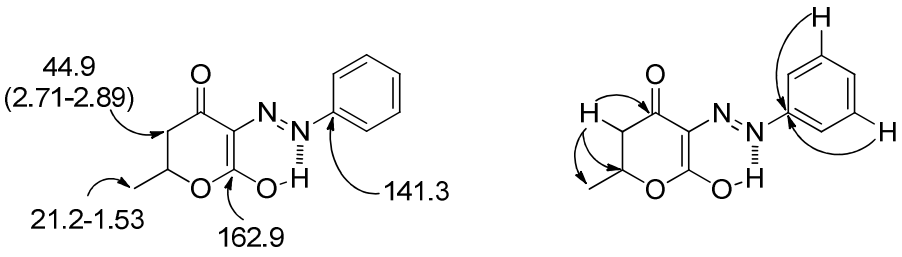

11

Fig. 7 a. Selected ^{1}H and ^{13}C NMR chemical shifts (right), **b.** HMBC correlations (left) for compound **11**

The spectra of the studied compounds of the second series provide additional evidence that they have the azo structures **T1** and **T4** (EAK and KAE) rather than the hydrazone structures **T2** and **T3** (KHK1 and KHK2). For example ^{1}H NMR spectrum of **11** in deuterated dimethyl sulfoxide exhibits two signals at 13.88 and 15.16 ppm with nearly equal integration ratio. Other compounds in these series show similar patterns.

2.4. Antimicrobial activity

Antibacterial activity was tested *in vitro* against Gram-positive and Gram-negative bacteria, using established drugs as standards. Both series of azodyes, **5** – **10** and new products **11** – **15**,

were screened for antimicrobial activity qualitatively by measuring the diameter of the clear inhibition zones (expressed in mm) around the paper discs using a transparent ruler, and quantitatively by determination of the minimum inhibitory concentrations (MICs), which are defined as the lowest concentration of compounds which visibly prevents the growth of bacteria.

2.4.1. Determination of inhibition zones

All synthesized compounds **5** – **15** exerted significant inhibitory activity against the growth of tested bacterial strains. As shown in Table 2, the diameter (mm) of inhibition zone values of tested compounds **5** – **15** against different strains ranged between 10 and 25 mm. Values of positive control, trimethoprim-sulfamethoxazole, were between 18 and 22 mm for both clinical and reference strains of *E. coli* and *S. aureus,* while *P. aeruginosa* strains were resistant to this antibiotic. The resistance shown by clinical *P. aeruginosa* to the synthesized compounds **5** – **9** and **15**, and to the selected reference antibiotic, is not surprising as these bacteria are well known for being resistant to a wider range of antibiotics than most of other bacteria. Interestingly, it is remarkable that this strain of *P. aeruginosa* was sensitive to other dyes, exceptional those derived from hydrogenated derivative of the 4-hydroxy-6-methyl-2H-pyran-2-one **11** – **14**. (Table 2)

Table 2.

Antibacterial screening data for inhibition zones of compounds **5** – **10** and new synthesized dyes **11** – **15** against different bacterial strains.

	Antimicrobial activity (zone of inhibition in mm)					
	Reference strains			Clinical strains		
	Gram+	Gram-		Gram+	Gram-	
Dye	*S.a.*	*E.c.*	*P.a.*	*S.a. 75*	*E.c. 10*	*P.a. 260*

5	11	15	18	16	17	0
6	15	10	16	15	20	0
7	12	0	14	0	16	0
8	16	16	19	18	17	0
9	0	20	18	15	20	0
10	16	18	18	16	14	18
11	25	18	19	17	20	17
12	19	17	17	12	19	15
13	16	19	19	15	18	20
14	18	18	16	13	22	19
15	21	20	17	14	20	0
Control	22	20	0	20	18	0

S.a.: *S. aureus*; *E.c.*: E coli; *P.a.*: *P. aeruginosa*

It should be noted that the concentration of the dyes used in the assays ranged between 0.5 and 512 µg/mL, and all compounds exhibited good growth inhibition of bacteria at different concentration as mentioned in Table 3. For example, compounds **9** and **15** have the best inhibition of growth of *E. coli* reference strain at 8 µg/mL with an inhibition zone diameter of 20 mm, while compound **14** has the best activity against *E. coli* clinical strain at 2 µg/mL with inhibition zone diameter of 22 mm. For reference strain of *S. aureus*, the best activity was detected for compounds **10** and **11** at 128 and 256 µg/mL with inhibition zone diameters of 16 and 25 mm, respectively. It is also noteworthy that *P. aeruginosa* was much more sensitive to compounds **8** and **13** for the reference strain at the same concentration (4 µg/mL) with inhibition zone diameters of 19 and 20 mm respectively whereas the clinical strain was much sensitive to **10** and **13** at 1 and 32 µg/mL with inhibition zone diameters of 18 and 20 mm, respectively. It should be also noted that the concentrations of the dyes giving the best

activities were much lower than that of the standard antibiotic (25 μg/mL). Nevertheless, the dyes at these lower concentrations seem to have similar levels of antibiotic activity (Table 3).

2.4.2. Determination of Minimum Inhibitory Concentrations

The data presented in Table 4 indicated that the substitution in phenyl ring exerted significant influence on the antibacterial profile. Interestingly, compounds with methoxy-substituted ring are found to be more active compounds in the respective series compared to the compounds bearing other groups. It is apparent that different derivatives exhibit appropriate MIC values against different strains of bacteria. For instance, compound **9** has excellent activity against both reference and clinical strains of *E. coli* with MIC values of 2 and 32 μg/mL, respectively,

Table 3.

Concentration and diameter of inhibition zone of compounds displaying the best antibacterial activity.

	Strains	**Dyes**	**Concentration (μg/ml)**	**Inhibition zone diameter(mm)**
	S. aureus	**10**	128	16
		11	256	25
		Control	25	22
Reference	*E. coli*	**9**	8	20
		15	8	20
		Control	25	20
	P. aeruginosa	**8**	4	19
		13	4	20
		Control	25	0
	S. aureus 75	**8**	4	18

		11	32	17
		Control	25	20
Clinical	*E. coli 10*	**9**	0.5	20
		14	2	22
		Control	25	20
	P. aeruginosa 260	**10**	1	18
		14	256	19
		Control	25	0

whereas product **10** showed significant inhibition against both reference and clinical *S. aureus* and *P. aeruginosa* strains, with MIC values 128 μg/mL and 256 μg/mL, respectively. More interesting results were obtained with the new synthesized series of compounds **11 – 15** with lower MIC values compared with the ones obtained within the first series of dyes **5 – 10**. Exceptional activities against reference and clinical *E. coli* strains were observed for compound **15** while for compound **14** only the clinical strain of *E. coli* was sensitive at the same MIC value of 1 μg/mL. Excellent activities against reference *S. aureus* and *P. aeruginosa* strains were observed for compounds **15** and **14** with MIC values of 16 and 32 μg/mL, respectively. Compared to methoxy-substituted compounds, both clinical *S. aureus* and *P. aeruginosa* strains showed more sensitivity to dyes with unsubstituted and nitro-substituted ring **11** and **13** with respective MIC values of 512 and 64 μg/mL.

Table 4.

In vitro antibacterial activity data in MIC (μg/ml) of tested compounds **5** – **10** and newly synthesized dyes **11 – 15** against different microbial species**.**

	Minimum Inhibitory Concentrations (μg/ml)	
	Reference strains	**Clinical strains**

	Gram +	Gram -		Gram +	Gram -	
Compound	***S.a.***	***E.c.***	***P.a.***	***S.a. 75***	***E.c. 10***	***P.a. 260***
5	11	128	256	512	512	R
6	15	R	512	512	256	R
7	12	R	512	R	128	R
8	16	2	512	512	32	R
9	0	8	256	512	64	512
10	16	8	128	256	512	256
11	25	128	128	512	4	64
12	19	2	64	R	8	64
13	16	8	64	512	32	64
14	18	16	32	R	1	256
15	21	1	64	R	1	512

S.a.: *S. aureus*; *E.c.*: *E coli*; *P.a.*: *P. aeruginosa*

3. Experimental

3.1. Measurements

Melting points were determined on a Stuart scientific SPM3 apparatus fitted with a microscope and the values reported in °C are uncorrected. Absorption spectra were determined on Jasco V-630 Bio UV spectrometer. FT-IR spectra were recorded on Magna-IR 550 spectrometer apparatus. NMR spectra were recorded with a Bruker Advance 1 spectrometer [400 MHz (^{1}H) and 100 MHz (^{13}C)] or a Bruker AH 300 FT spectrometer [300 MHz (^{1}H) and 75 MHz (^{13}C)]. Chemical shifts are expressed in parts per million (ppm) downfield from TMS. Data are reported as follows: chemical shift [multiplicity (s: singlet, d: doublet, t: triplet, m: multiplet), coupling constants (*J*) in Hertz (Hz), integration]. Shifts of ^{1}H and ^{13}C NMR spectra were calibrated against the solvent residual isotopic peak as internal

reference. Reference peaks for the NMR spectra in $(CD_3)_2SO$ are 2.50 (^1H) and 39.52 (^{13}C) and for $CDCl_3$ 7.26 (^1H) and 77.16 (^{13}C). Mass spectra were determined on a Waters Micromass LCT Premier Q-TOF Mass spectrometer coupled with a Waters Alliance HPLC.

3.2. Materials

All the chemicals and solvents used in this study were purchased from Fluka and Sigma Aldrich. Grades of chemicals were as follow: 4-hydroxy-6-methyl-2-pyrone: 98%, aniline **3a**: ≥99.5%, 4-bromoaniline **3b** and 2,3-dimethoxyaniline **3f:** for synthesis, 4-nitroaniline **3c** and *p*-anisidine **3d:** ≥99%, 2,4-dimethoxyaniline **3e:** 97%, sodium nitrite: ≥97.0%, hydrochloric acid: 37%, sodium acetate: >99%.

The reference strains *Staphylococcus aureus* [ATCC 25923], *Escherichia coli* [ATCC-25922] and *Pseudomonas aeruginosa* [ATCC-27853] used were obtained from Pasteur Institute, Algiers. Clinical strains *S. aureus*, *E. coli* and *P. aeruginosa* used in this study were isolated from different samples: pus, urine and blood. Identification of the bacterial strains was made on cultural and biochemical characters.

3.3. Chemistry

Compounds **1** and **2** were prepared (Scheme 2) according to known procedures [24,33,34].

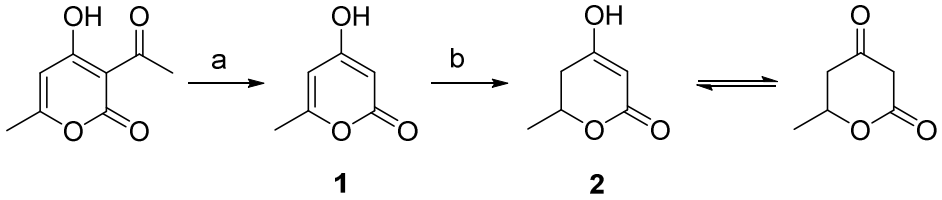

a: H_2SO_4, 140 °C, 20 min; b: H_2/ Pd-C, RT, 24 h.

Scheme 2. Preparation of TAL **1** and DHTAL **2**.

Azo derivatives **5** – **15** were synthesized by the azo-coupling reactions of substituted benzene diazonium salts **4a** – **f** with 4-hydroxy-6-methyl-2H-pyran-2-one (**1**) and 4-hydroxy-6-methyl-5,6-dihydro-2H-pyran-2-one (**2**), respectively.

3.3.1. General procedure of diazotation

303 Aromatic amine **3a** – **f** (6 mmol) was dissolved in a freshly prepared 10% solution of
304 concentrated hydrochloric acid (10 mL) then cooled to 0 – 5 °C using an ice-bath. A solution
305 of sodium nitrite ($NaNO_2$, 0.45 g, 6 mmol) in water (10 mL) was added dropwise while the
306 temperature was maintained below 5 °C. The resulting mixture was stirred for 30 min in an
307 ice bath (Scheme 3).

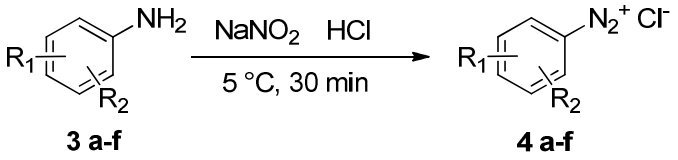

3 a-f **4 a-f**

a: $R_1 = R_2 = H$
b: $R_1 = H$, $R_2 = p$-Br
c: $R_1 = H$, $R_2 = p$-NO_2
d: $R_1 = H$, $R_2 = p$-OCH_3
e: $R_1 = o$-OCH_3, $R_2 = p$-OCH_3
f: $R_1 = o$-OCH_3, $R_2 = m$-OCH_3

308

309 **Scheme 3.** Preparation of diazonium salts **4a** – **f**

310 *3.3.2. Preparation of dyes*

311 When diazotation was complete, as described above, the resulting substituted aryl-diazonium
312 salts **4a** – **f** were used to prepare the target molecules **5** – **15** as described below (Schemes 4
313 and 5). The two tautomeric forms are described as they appear from the spectra as a mixture
314 of Major (M) and minor (m) products. The selected physical properties of the synthesized
315 dyes **5** – **15** were measured and listed in Table 5.

316 **Table 5.**

317 Physical properties and yields of synthesized dyes

Dye	R_1, R_2	**m.p.** (°C)	**λmax** (nm) in CH_2Cl_2	**Color**	**Yield** (%)	**Ref**
5	H, H	183-185	418.6	Orange	83	[35]
6	H, 4-Br	235-237	424.4	Brick	50	this work
7	H, 4-NO_2	245-247	417.2	Yellow	5	this work
8	H, 4-OCH_3	192-194	443.8	Orange	75	[35]

9	2,4-OCH_3	218-220	462.6	Orange	33	this work
10	2,5-OCH_3	175-177	461.0	Red	72	this work
11	H, H	156	387.8	Yellow	29	[36]
12	H, 4-Br	173	400.4	Brown	50	this work
13	H, 4-NO_2	201	393.6	Yellow	37	this work
14	H, 4-OCH_3	150-153	418.0	Purple	30	[36]
15	2,4-OCH_3	180	436.0	Brown	100	this work

*3.2.2.1. Synthesis of (E)-4-Hydroxy-6-methyl-3-(aryldiazenyl)-2H-pyran-2-ones (or 3-(2-(aryl)hydrazono)-6-methyl-3H-pyran-2,4-diones) (**5** – **10**)*

The substituted aryl-diazonium salts (**4a** – **f**) were added dropwise to a mixture of 4-hydroxy-6-methyl-2H-pyran-2-one (**1**) (TAL, 0.63 g, 5 mmol) in water (10 mL) and sodium acetate (1 g, 3 mmol). The reaction mixture was stirred for 2 h at 0 – 5 °C. The obtained precipitate was filtered off, washed with cold water, dried and recrystallized from ethanol to give the pure compounds **5** – **10** (Scheme 4).

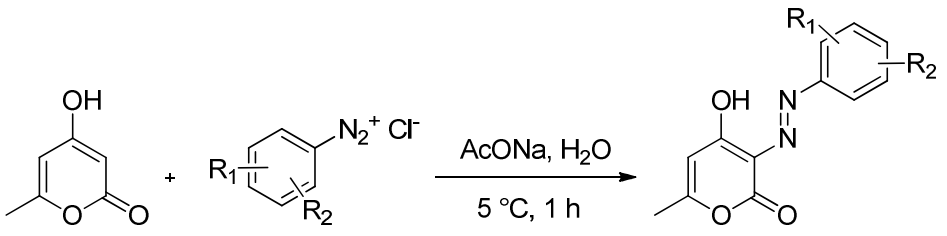

a: $R_1 = R_2 = H$
b: $R_1 = H$, $R_2 = p$-Br
c: $R_1 = H$, $R_2 = p$-NO_2
d: $R_1 = H$, $R_2 = p$-OCH_3
e: $R_1 = o$-OCH_3, $R_2 = p$-OCH_3
f: $R_1 = o$-OCH_3, $R_2 = m$-OCH_3

5: $R_1 = R_2 = H$
6: $R_1 = H$, $R_2 = p$-Br
7: $R_1 = H$, $R_2 = p$-NO_2
8: $R_1 = H$, $R_2 = p$-OCH_3
9: $R_1 = o$-OCH_3, $R_2 = p$-OCH_3
10: $R_1 = o$-OCH_3, $R_2 = m$-OCH_3

Scheme 4. Synthetic route for the preparation of azo dyes **5 – 10**.

(*E*)-4-Hydroxy-6-methyl-3-(phenyldiazenyl)-2H-pyran-2-one (or 6-methyl-3-(2-phenylhydrazono)-3*H*-pyran-2,4-dione) (5): Orange solid (0.805g, 70%). FT-IR (KBr, υ cm^{-1}): 3030, 2980,1759, 1650, 1509. ^{1}H NMR (300 MHz, $CDCl_3$) δ ppm: 2.23 (s, 3H), 5.83 (s, 1H), 7.28 – 7.34 (m, 1H), 7.40 – 7.49 (m, 2H), 7.56 – 7.64 (m, 2H), 14.15 (bs, NH_M), 16.31 (bs, OH_M). ^{13}C NMR (75 MHz, $CDCl_3$) δ: 20.5 (C_7), 107.6 (C_5), 117.9 (C_9, C_{13}), 122.0 (C_3), 128.3 (C_{11}), 129.8 (C_{10}, C_{12}), 140.5 (C_8), 159.6 (C_2), 166.7 (C_4), 181.0 (C_6). HRMS (ESI) m/z calcd for $C_{12}H_{11}N_2O_3$ ($[M+H]^+$): 231.0770; found: 231.0775 (100%) and calcd for $C_{12}H_{11}N_2O_3Na$ ($[M+Na]^+$): 253.0589; found: 253.0598 (83%).

(*E*)-3-((4-Bromophenyl)diazenyl)-4-hydroxy-6-methyl-2H-pyran-2-one (or 3-(2-(4-bromophenyl)hydrazono)-6-methyl-3*H*-pyran-2,4-dione (6): Brick solid (1.228 g, 80%). FT-IR (KBr, υ cm^{-1}): 3103, 2960, 1738, 1625, 1512. ^{1}H NMR (300 MHz, $CDCl_3$) δ ppm: 2.24 (s, 1H), 5.85 (s, 1H), 7.45 – 7.52 (m, 2H), 7.54 – 7.59 (m, 2H), 14.08 (bs, NH_M), 16.26 (bs, OH_M). ^{13}C NMR (75 MHz, $CDCl_3$) δ ppm: 20.7 (C_7), 107.6 (C_5), 119.5 (C_9, C_{13}), 121.8 (C_3), 122.5 (C_{11}), 133.0 (C_{10}, C_{12}), 139.7 (C_8), 159.6 (C_2), 167.2 (C_4), 181.3 (C_6). HRMS (ESI) m/z calcd for $C_{12}H_{10}BrN_2O_3$ ($[M+H]^+$, ^{79}Br): 308.9875; found: 308.9872 (100%) and calcd for $C_{12}H_{10}BrN_2O_3Na$ ($[M+Na]^+$, ^{79}Br): 330.9694; found: 330.9688 (50%).

(*E*)-4-Hydroxy-6-methyl-3-((4-nitrophenyl)diazenyl)-2H-pyran-2-one (or 6-methyl-3-(2-(4-nitrophenyl)hydrazono)-3*H*-pyran-2,4-dione) (7): Yellow solid (1.031 g, 75%). FT-IR (KBr, υ cm^{-1}): 3084, 2935, 1758, 1650, 1501. ^{1}H NMR (300 MHz, $CDCl_3$) δ ppm: 2.21 (s, 3H), 5.98 (s, 1H), 7.83 – 7.90 (m, 2H), 8.25 – 8.31 (m, 2H), 14.35 (bs, NH_m), 16.44 (bs, OH_M). HRMS (ESI) m/z calcd for $C_{12}H_{10}N_3O_5$($[M+H]^+$): 276.0620; found 276.0620 (33%) and calcd for $C_{12}H_9N_3O_5Na$ ($[M+Na]^+$): 298.0440; found 298.0444 (5%).

***(E)*-4-Hydroxy-3-((4-methoxyphenyl)diazenyl)-6-methyl-2H-pyran-2-one (or 3-(2-(4-methoxyphenyl)hydrazono)-6-methyl-3*H*-pyran-2,4-dione) (8)**: Orange solid (0.780 g,

60%).FT-IR (KBr, υ cm^{-1}): 3075, 2839, 1731, 1600, 1498. ^{1}H NMR (300 MHz, $CDCl_3$) δ, ppm: 2.23 (d, *J* = 0.6 Hz, 3H), 3.85 (s, 3H), 5.83 (d, *J* = 0.6 Hz, 1H), 6.92 – 7.00 (m, 2H), 7.54 – 7.62 (m, 2H), 14.31 (bs, NH_m), 16.48 (bs, OH_M). ^{13}C NMR (75 MHz, $CDCl_3$) δ ppm: 20.4 (C_7), 55.7 (OCH_3), 107.5 (C_5), 115.1 (C_{10}, C_{12}), 119.7 (C_9, C13), 122.03 (C_3), 134.1 (C_8), 159.0 (C_2), 160.0 (C_4), 166.1 (C_{11}), 181.2 (C_6). HRMS (ESI) m/z calcd for $C_{13}H_{13}N_2O_4$ ($[M+H]^+$): 261.0875; found: 261.0876 (100%) and calcd for $C_{13}H_{12}N_2O_4Na$ ($[M+Na]^+$): 283.0695; found: 283.0693 (75%).

(*E*)-3-((2,4-dimethoxyphenyl)diazenyl)-4-hydroxy-6-methyl-2H-pyran-2-one (or 3-(2-(2,4-dimethoxyphenyl)hydrazono)-6-methyl-3*H*-pyran-2,4-dione) (9): Orange solid (0.826 g, 57%). FT-IR (KBr, υ cm^{-1}): 3050, 2940, 1739, 1620, 1511. ^{1}H NMR (300 MHz, $CDCl_3$) δ ppm: 2.23 (s, 3H), 3.85 (s, 3H), 3.97 (s, 3H), 5.82 (s, 1H), 6.51 (d, *J* = 2.4 Hz, 1H), 6.58 (dd, *J* = 9.0, 2.4 Hz, 1H), 7.94 (d, *J* = 9.0 Hz, 1H), 14.37 (bs, NH_m), 16.34 (bs, OH_M). ^{13}C NMR (75 MHz, $CDCl_3$) δ ppm: 20.8 (C_7), 56.1 (OCH_3), 56.6 (OCH_3), 99.0 (C_{10}), 106.6 (C_{12}), 108.0 (C_5), 118.9 (C_{13}), 122.0 (C_3), 124.2 (C_8), 151.5 (C_9), 161.0 (C_2), 161.5 (C_{11}), 165.8 (C_4), 180.6 (C_6). HRMS (ESI) m/z calcd for $C_{14}H_{15}N_2O_5$ ($[M+H]^+$): 291.0981; found 291.0980 (100%) and calcd for $C_{14}H_{14}N_2O_5Na$ ($[M+Na]^+$): 313.0800; found 313.0793 (33%).

(*E*)-3-((2,5-Dimethoxyphenyl)diazenyl)-4-hydroxy-6-methyl-2H-pyran-2-one (or 3-(2-(2,5-dimethoxyphenyl)hydrazono)-6-methyl-3*H*-pyran-2,4-dione (10): Red solid (0.681 g, 47%). FT-IR (KBr, υ cm^{-1}): 3072, 2841, 1749, 1610, 1498. ^{1}H NMR (300 MHz, $CDCl_3$) δ ppm: 2.23 (s, 3H), 3.86 (s, 3H), 3.97 (s, 3H), 5.83 (d, *J* = 0.7 Hz, $1H_M$), 5.98 (s, $1H_m$), 6.82 (dd, *J* = 9.0, 2.9 Hz, 1H), 6.90 (d, *J* = 9.0 Hz, 1H), 7.50 (d, *J* = 2.9 Hz, 1H), 14.37 (bs, NH_m), 16.34 (bs, OH_M). ^{13}C NMR (75 MHz, $CDCl_3$) δ ppm: 20.6 (C_7), 56.2 (OCH_3 at C_{12}), 56.6 (OCH_3 at C_9), 101.4 (C_{11}), 107.8 (C_5), 112.7 (C_{13}), 115.7 (C_{10}), 125.5 (C_3), 130.3 (C_8), 144.2 (C_9), 154.9 (C_{12}), 160.1 (C_2), 166.1 (C_4), 180.6 (C_6). HRMS (ESI) m/z calcd for $C_{14}H_{15}N_2O_5$

([M+H]$^+$): 291.0981; found: 291.0990 (100%) and calcd for $C_{14}H_{14}N_2O_5Na$ ([M+Na]$^+$): 313.0800; found: 313.0806 (72%).

*3.2.2.2. Synthesis of (E)-4-hydroxy-6-methyl-3-(aryldiazenyl)-5,6-dihydro-2H-pyran-2-one (or 3-(2-(aryl) hydrazono)-6-methyl-dihydro-3H-pyran-2,4-diones (**11** – **15**).*

The obtained diazo liquor (**4a** – **e**) was added to a vigorously stirred mixture of 4-hydroxy-6-methyl-5,6-dihydro-2H-pyran-2-one (**2**) (0.64 g, 5 mmol) in water (10 mL) and sodium acetate (1 g, 3 mmol) in water (10 mL). The mixture was then stirred for 2 h at 0 – 5 °C. After completion of the reaction, the resulting solid was filtered, washed with cold water and dried. Recrystallization from ethanol gave pure solid (**11** –**15**) (Scheme 5).

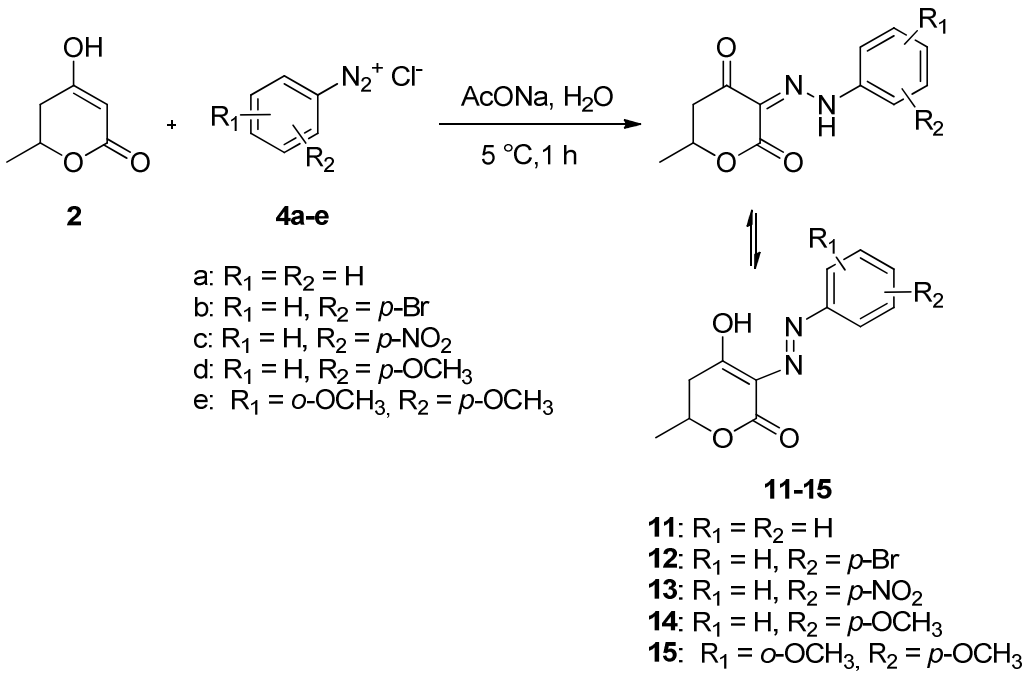

Scheme 5. Synthetic route for the preparation of azo dyes **11** – **15**.

(*E*)-4-hydroxy-6-methyl-3-(phenyldiazenyl)-5,6-dihydro-2H-pyran-2-one (or 6-methyl-3-(2-phenylhydrazono)-dihydro-3*H*-pyran-2,4-dione) (11): Yellow solid (0.986 g, 85%). FT-IR (KBr, υ cm^{-1}): 3070, 2940, 1710, 1600, 1511. ^{1}H NMR (300 MHz, $CDCl_3$) δ ppm: 1.53 (d, *J* = 6.4 Hz, 3H), 2.71 – 2.89 (m, 2H), 4.68 – 4.83 (m, 1H), 7.24 – 7.31 (m, 1H), 7.43 (t, *J* = 7.9 Hz, 2H), 7.55 (t, *J* = 7.7 Hz, 2H), 13.88 (bs, 1H, NH_m), 15.16 (bs, 1H, OH_M). ^{13}C NMR (75 MHz, $CDCl_3$) δ ppm: 21.2 (C_{7M}), 44.9 (C_{5M}), 45.2 (C_{5m}), 71.3 (C_{6M}), 72.9 (C_{6m}), 117.7

(C_{9M}, C_{13M}), 117.8 (C_{9m}, C_{13m}), 121.5 (C_{3m}), 122.9 (C_{3M}), 127.5 (C_{11m}), 128.0 (C_{11M}), 130.0 (C_{10M}, C_{12M}), 130.1 (C_{10m}, C_{12m}),141.0 (C_{8m}), 141.1 (C_{8M}), 163.7 (C_{2M}), 165.4 (C_{2m}), 188.5 (C_{4m}), 192.2 (C_{4M}). HRMS (ESI) m/z calcd for $C_{12}H_{13}N_2O$ ($[M+H]^+$): 233.0926; found: 233.0921 (100%).

(*E*)-3-((4-Bromophenyl)diazenyl)-4-hydroxy-6-methyl-5,6-dihydro-2H-pyran-2-one (or 3-(2-(4-bromophenyl)hydrazono)-6-methyl-dihydro-3*H*-pyran-2,4-dione) (12): Brown solid (0.899 g, 58%). FT-IR (KBr, υ cm^{-1}): 3090, 2986, 1693, 1630, 1508.^{1}H NMR (300 MHz, DMSO) δ, ppm: 1.37 (d, *J* = 6.3 Hz, 3H), 2.73 (dd, *J* = 17.0, 3.2 Hz, 1H), 2.86 (dd, *J* = 17.0, 10.6 Hz, 1H), 4.74 – 4.92 (m, 1H), 7.55 – 7.67 (m, 4H), 13.25 (bs, 1H, NH_m), 14.42 (bs, 1H, OH_M). ^{13}C NMR (75 MHz, DMSO) δ ppm: 20.3 (C_{7m}), 20.8 (C_{7M}), 44.5 (C_{5M}), 44.8 (C_{5m}), 70.9 (C_{6M}), 72.3 (C_{6m}), 118.4 (C_{11m}), 118.9 (C_{11M}), 119.3 (C_{9M}, C_{13M}), 120.0 (C_{9m}, C_{13m}), 123.9 (C_{11M}), 124.1 (C_{3M}), 132.9 (C_{10M}, C_{12M}), 133.1 (C_{10m}, C_{12m}), 141.1 (C_{8m}), 141.3 (C_{8M}), 162.9 (C_{2M}), 169.0 (C_{2m}), 189.0 (C_{4m}), 192.6 (C_{4M}). HRMS (ESI) m/z calcd for $C_{12}H_{12}BrN_2O_3$ ($[M+H]^+$,^{79}Br): 311.0031; found 311.0031 (100%).

(*E*)-4-Hydroxy-6-methyl-3-((4-nitrophenyl)diazenyl)-5,6-dihydro-2H-pyran-2-one (or 6-methyl-3-(2-(4-nitrophenyl)hydrazono)-dihydro-3*H*-pyran-2,4-dione) (13): Yellow solid (1.149 g, 83%). FT-IR (KBr, υ cm^{-1}): 3060, 2960, 1715, 1625, 1504.^{1}H NMR (300 MHz, $CDCl_3$) δ ppm: 1.54 (d, *J* = 6.0 Hz, 3H), 2.71 – 2.90 (m, 2H), 4.68 – 4.85 (m, 1H), 7.40 – 7.57 (m, 4H), 13.82 (s, 1H, NH_m), 15.08 (s, 1H, OH_M). ^{13}C NMR (75 MHz, $CDCl_3$) δ ppm: 21.3 (C_{7m}), 21.6 (C_{7M}), 45.3 (C_{5M}), 45.6 (C_{5m}), 71.7 (C_{6M}), 73.4 (C_{6m}), 119.5 (C_{9M}, C_{13M}), 120.0 (C_{9m}, C_{13m}), 121.0 (C_{11m}), 121.5 (C_{11M}), 122.3 (C_{3m}), 123.6 (C_{3M}), 133.5 (C_{10M}, C_{12M}), 133.6 (C_{10m}, C_{12m}), 140.5 (C_{8m}), 140.6 (C_{8M}), 163.9 (C_{2M}), 165.6 (C_{2m}), 188.1 (C_{4m}), 192.9 (C_{4M}). HRMS (ESI) m/z calcd for $C_{12}H_{12}N_3O_5$ ($[M+H]^+$): 278.0777; found: 278.0781 (100%).

(*E*)-4-Hydroxy-3-((4-methoxyphenyl)diazenyl)-6-methyl-5,6-dihydro-2H-pyran-2-one (or 3-(2-(4-methoxyphenyl)hydrazono)-6-methyl-dihydro-3H-pyran-2,4-dione) (14):

Purple solid (0.589 g, 45%).FT-IR (KBr, υ cm^{-1}): 3078, 2909, 1708, 1630, 1510.^{1}H NMR (300 MHz, $CDCl_3$) δ, ppm: 1.53 (d, *J* = 6.2 Hz, 3H), 2.68 – 2.86 (m, 2H), 3.85 (s, 3H), 4.65 – 4.82 (m, 1H), 6.93 – 6.70 (m, 2H), 7.47 – 7.53 (m, 2H), 14.03 (s, 1H, NH_m), 15.41 (s, 1H, OH_M). ^{13}C NMR (75 MHz, $CDCl_3$) δ ppm: 21.2 (C_7), 44.7 (C_{5M}), 45.1 (C_{5m}), 56.0 (C_{14}), 71.3 (C_{6M}), 72.9 (C_{6m}), 115.4 (C_9, C_{13}), 119.4 (C_{10}, C_{12}), 120.6 (C_{3m}), 122.1 (C_{3M}), 134.5 (C_{8M}), 134.6 (C_{8m}), 159.4 (C_{11m}), 159.8 (C_{11M}), 164.1 (C_{2M}), 165.7 (C_{2m}), 188.5 (C_{4m}), 191.7 (C_{4M}). HRMS (ESI) m/z calcd for $C_{13}H_{15}N_2O_4$ ($[M+H]^+$: 263.1032; found: 263.1028 (100%).

(*E*)-3-((2,4-Dimethoxyphenyl)diazenyl)-4-hydroxy-6-methyl-5,6-dihydro-2H-pyran-2-one (or 3-(2-(2,4-dimethoxyphenyl)hydrazono)-6-methyl-dihydro-3H-pyran-2,4-dione (15): Brown solid (0.580 g, 40%). FT-IR (KBr, υ cm^{-1}): 3079, 2900, 1706, 1625, 1505.^{1}H NMR (300 MHz, $CDCl_3$) δ ppm: 1.51 (d, *J* = 6.4 Hz, 3H), 2.66 – 2.85 (m, 2H), 3.83 (s, $3H_m$), 3.84 (s, $3H_M$), 3.94 (s, $3H_m$), 3.96 (s, $3H_M$), 4.67 – 4.76 (m, 1H), 6.50 (s, 1H), 6.51 – 6.59 (m, 1H), 7.84 (d, *J* = 8.9 Hz, $1H_m$), 7.88 (d, *J* = 8.8 Hz, $1H_M$), 14.16 (bs, 1H, NH_m), 15.47 (bs, 1H, OH_M). ^{13}C NMR (75 MHz, $CDCl_3$) δ, ppm: 21.3 (C_7), 44.6 (C_{5M}), 45.0 (C_{5m}), 56.1 (C_{14}), 56.4 (C_{15}), 71.3 (C_{6M}), 72.7 (C_{6m}), 99.1 (C_{10}), 106.1 (C_{12m}), 106.1 (C_{12M}), 118.2 (C_{13m}), 118.4 (C_{13M}), 120.1 (C_{3m}), 122.4 (C_{3M}), 124.1 (C_{8M}), 124.3 (C_{8m}), 150.7 (C_{9M}), 150.9 (C_{9m}), 160.3 (C_{11m}), 160.7 (C_{11M}), 164.6 (C_{2M}), 165.6 (C_{2m}), 188.8 (C_{4m}), 190.8 (C_{4M}). HRMS (ESI) m/z calcdfor $C_{14}H_{17}N_2O_5$($[M+H]^+$): 293.1137; found: 293.1142 (41%) and calcd for $C_{14}H_{16}N_2O_5Na$ ($[M+Na]^+$): 315.0957; found: 315.0952 (100%).

3.4. Biology

3.4.1. Bacterial strains

The antimicrobial activity of the synthesized compounds was evaluated *in vitro* versus three reference strains: *Staphylococcus aureus* [ATCC-25923] (S.a.) as Gram positive bacterium; *Escherichia coli* [ATCC-25922] (E.c.) and *Pseudomonas aeruginosa* [ATCC-27853] (P.a.) as Gram negative bacteria and three clinical strains isolates from urine, blood and pus:

Staphylococcus aureus 75 (S2), *Escherichia coli* 10 (S1), and *Pseudomonas aeruginosa* 260 (S3).

3.4.2. Antimicrobial activity determination

All compounds (**5** –**15**) were dissolved in acetone and further serial ten-fold dilutions were made in a concentration range from 0.5 to 512 µg/mL in order to prepare the working solutions used for determination of inhibition zones as well as for determination of minimal inhibitory concentrations (MIC). Trimethoprime-Sulfamethoxazole was used as reference standard at a concentration of 25 µg/mL in order to validate methodology and also for comparison of antimicrobial activities.

3.4.2.1 Determination of inhibition zones

All synthesized compounds (**5** – **15**) were examined for antibacterial activity against different Gram-positive and Gram-negative strains of bacteria. Inhibition zones of the best compounds (**8** – **11**, **13** – **15**) were performed with the disk diffusion method using nutrient agar medium [23,29]. The Mueller–Hinton agar medium was autoclaved for 30 min, poured under aseptic conditions in each sterilized Petri dish, allowed to solidify and then inoculated with fresh subculture of a bacterial inocula prepared in physiological sterile water. Sterile 6 mm filter paper discs, impregnated with 20 µl of the different concentrations of tested compounds were then placed on agar plates and the cultures were incubated at 37 °C for 24 h for bacterial growth. Disks embedded with acetone were used as a negative control. Inhibition zones formed on the medium were evaluated in millimeter (mm).

*3.4.2.2 Determination of minimal inhibitory concentration***s**

The minimum inhibitory concentration (MIC) values of compounds **5 – 15** were determined by broth micro-dilution method [22,29-30]. The microbial suspensions were prepared in Mueller–Hinton broth from test organisms sub-cultured on nutrient agar. The serial prepared solutions ranging from concentration 0.5 to 512 µg/mL were inoculated with fresh bacterial

inoculums and incubated at 37 °C for 24 h. The results were recorded according to the presence or absence of bacteria growth comparatively to the controls.

Conclusions

In this study, some known and unknown azo disperse dyes **5** – **15** were prepared by classical method of azo coupling reaction using as nucleophilic partner TAL **1** and DHTAL **2**. The synthesized dyes were characterized by FT-IR, electronic absorption spectra in UV and visible regions, ^{1}H, ^{13}C and 2D NMR and mass spectroscopy. The solvent polarities and substituents effects on the photophysical properties of dyes were evaluated. The spectroscopic data of the synthesized dyes revealed that these compounds exist as mixtures of two tautomeric azo and hydrazo forms which are in equilibrium, the azo one being major. Furthermore, measurement of antibacterial activity demonstrated that the dyes, at lower concentration, showed similar activities against *E. coli* and *S. aureus* as those shown by the control antibiotic, while *P. aeruginosa* strains were sensitive to synthesized molecules compared to control antibiotic. The effect of these dyes on microbes therefore deserves further examination.

Acknowledgements

The authors thank Karine Leblanc (Faculty of Pharmacy, Châtenay-Malabry, France) for high resolution mass spectra and Camille Dejean for NMR spectra. The Ministry of Higher Education and Scientific Research (Algeria), the Centre National de la Recherche Scientifique (CNRS, France), the Ministry of Education, Research and Technology (France), IPSIT and LabEx LERMIT (ANR-10-LABX-33) are gratefully acknowledged for financial support.

References

[1] Stead, CV. Azo Dyes (Chapter VI) in The Chemistry of Synthetic Dyes, Volume III, Venkataraman K. Ed. Academic Press, New York and London, 1970, pp 303–369.

[2] Zhi-Gang Y, Chun-Xia Z, De-Feng Z, Freeman HS, Pei-Tong C, Jie H. Monoazodyes based on 5,10-dihydrophenophosphazine, Part 2: Azo acid dyes. Dyes and Pigments, 2009, 81, 137–43. DOI: 10.1016/j.dyepig.2008.09.021

[3] Gregory P. High-Technology Applications of Organic Colorants. In Topics in Applied Chemistry, Katritzky AR, Sabongi GJ, Eds, New York, Plenum press, 1991, Chapters 3-5, pp 27-52. DOI: 10.1007/978-1-4615-3822-6

[4] Gregory P. Modern reprographics. Review of progress in coloration and related topics. 1994, 24, 1–16. DOI: 10.1111/j.1478-4408.1994.tb03763.x

[5] Chung, K-T. Azo dyes and human health: A review. Journal of Environmental Science and Health, Part C, 2016, 34(4), 233–261. DOI: 10.1080/10590501.2016.1236602

[6] Piao W, Hanaoka K, Fujisawa T, Takeuchi S, Komatsu T, Ueno T, Terai T, Tahara T, Nagano T, Urano Y. Development of an Azo-Based Photosensitizer Activated under Mild Hypoxia for Photodynamic Therapy. The Journal of the American Chemical Society, 2017, 139(39), 13713–13719. DOI: 10.1021/jacs.7b05019

[7] Mekkawi DE, Abdel-Mottaleb MSA. The interaction and photostability of some xanthenes and selected azo sensitizing dyes with TiO_2 nanoparticles. International Journal of Photoenergy, 2005, 7(2), 95–101. DOI: 10.1155/S1110662X05000140

[8] Bafana A, Devi SS, Chakrabarti T. Azo dyes: past, present and the future. Environmental Reviews 2011, 19, 350–370. DOI: 10.1139/a11-018

[9] Li Y, Patrick BO, Dolphin D. Near-Infrared Absorbing Azo Dyes: Synthesis and X-ray Crystallographic and Spectral Characterization of Monoazopyrroles, Bisazopyrroles and a Boron-Azopyrrole Complex. The Journal of Organic Chemistry, 2009, 74, 5237–5243. DOI: 10.1021/jo9003019

515 [10] Yazdanbakhsh MR, Mohammadi A. Synthesis, substituent effects and solvatochromic
516 properties of some disperse azo dyes derived from N-phenyl-2, 2′-iminodiethanol. Journal of
517 Molecular Liquids, 2009, 148(1), 35–39. DOI 10.1016/j.molliq.2009.06.001
518 [11] Albayrak C, Gumrukcuoglu IE, Odabas-oglu M, Iskeleli NO, Agar E. Synthesis,
519 spectroscopic, and molecular structure characterizations of some azo derivatives of 2-
520 hydroxyacetophenone. Journal of Molecular Structure, 2009, 932, 43–54. DOI:
521 10.1016/j.molstruc.2009.05.043
522 [12] Yazdanbakhsh MR, Abbasnia M, Sheykhan M, Ma'mani L. Synthesis, characterization
523 and application of new azo dyes derived from uracil for polyester fiber dyeing. Journal of
524 Molecular Structure, 2010, 977, 266–273. DOI: 10.1016/j.molstruc.2010.06.005
525 [13] Moradi Rufchahi EO, Ghanadzadeh Gilani A. Synthesis, characterization and
526 spectroscopic properties of some new azo disperse dyes derived from 4-
527 hydroxybenzo[h]quinolin-2-(1H)-one as a new synthesized enol type coupling component.
528 Dyes and Pigments, 2012, 95(3), 632–638. DOI: 10.1016/j.dyepig.2012.06.008
529 [14] Shawali AS, Harb NMS, Badahdah KO. A study of tautomerism in diazonium coupling
530 products of 4-hydroxycoumarin. Journal of Heterocyclic Chemistry, 1985, 22(5), 1397–1403.
531 DOI: 10.1002/jhet.5570220555
532 [15] Traven VF, Negrebetsky VV, Vorobjeva LI, Carberry EA. Keto-Enol Tautomerism,
533 NMR Spectra, and H-D Exchange of 4-Hydroxycoumarins. Canadian Journal of Chemistry,
534 1997, 75, 377-383. DOI: 10.1139/v97-043
535 [16] Yazdanbakhsh MR, Ghanadzadeh A, Moradi E. Synthesis of some new azo dyes derived
536 from 4-hydroxycoumarin and spectrometric determination of their acidic dissociation
537 constants. Journal of Molecular Liquids, 2007, 136, 165-168. DOI:
538 10.1016/j.molliq.2007.03.005

539 [17] Moradi-e-Rufchahi EO, Ghanadzadeh A. A study of Solvatochromism in diazonium
540 coupling products of 6-fluoro-4-hydroxyl-2-quinolone. Journal of Molecular Liquids, 2011,
541 160, 160–165. DOI: 10.1016/j.molliq.2011.03.011
542 [18] Yazdanbakhsh MR, Yousefi H, Mamaghani M, Moradi EO, Rassa M, Pouramir H,
543 Bagheri M. Synthesis, spectral characterization and antimicrobial activity of some new azo
544 dyes derived from 4,6-dihydroxypyrimidine. Journal of Molecular Liquids, 2012, 169, 21–26.
545 DOI: 10.1016/j.molliq.2012.03.003
546 [19] Shawali AS. Synthesis and tautomerism of aryl- and hetaryl-azo derivatives of bi- and
547 tri-heterocycles. Journal of Advanced Research, 2010, 1(4), 255-290. DOI:
548 10.1016/j.jare.2010.07.002
549 [20] Karci F, Ertan N. Hetarylazo disperse dyes derived from 3-methyl-1-(3,5-dipiperidino-*s*-
550 triazinyl)-5-pyrazolone as coupling component. Dyes and Pigments, 2002, 55, 99–108. DOI:
551 10.1016/j.molliq.2012.03.003
552 [21] Sener I, Karcı F, Ertan N, Kılıç E. Synthesis and investigations of the absorption spectra
553 of hetarylazo disperse dyes derived from 2,4-quinolinediol. Dyes and Pigments, 2006, 70,
554 143–148. DOI: 10.1016/j.dyepig.2005.05.003
555 [22] Mohammadi A, Reza Yazdanbakhsh M, Farahnak L. Synthesis and evaluation of
556 changes induced by solvent and substituent in electronic absorption spectra of some azo
557 disperse dyes, Spectrochimica Acta Part A: Molecular and Biomolecular Spectroscopy, 2012,
558 89, 238–242. DOI1/ 10.1016/j.saa.2011.12.062
559 [23] Sayed AZ, Aboul-Fetouh MS, Nassar HS. Synthesis, biological activity and dyeing
560 performance of some novel azo disperse dyes incorporating pyrazolo[1,5-a]pyrimidines for
561 dyeing of polyester fabrics, Journal of Molecular Structure, 2012, 1010, 146–151. DOI:
562 10.1016/j.molstruc.2011.11.046

563 [24] Ben Mohamed S, Rachedi Y, Hamdi M, Le Bideau F, Dejean C, Dumas F. An Efficient
564 Synthetic Access to Substituted Thiazolyl-pyrazolyl-chromene-2-ones from Dehydroacetic
565 Acid and Coumarin Derivatives by a Multicomponent Approach. European Journal of
566 Organic Chemistry, 2016, 2016, 2628–2636. DOI: 10.1002/ejoc.201600173
567 [25] Gangoué-Piéboji J, Eze N, Djintchui AN, Ngameni B, Tsabang N, Pegnyemb DE, Biyiti
568 L, Ngassam P, Koulla-Shiro S, Galleni M. The in-vitro antimicrobial activity of some
569 medicinal plants against β-lactam-resistant bacteria, Journal of Infection in Developing
570 Countries**,** 2009, 3, 671–680. DOI: 10.3855/jidc.77
571 [26] Hughes D, Karlén A, Discovery and preclinical development of new antibiotics, Upsala
572 Journal of Medical Sciences, 2014, 119(2), 162–169. DOI: 10.3109/03009734.2014.896437
573 [27] Diaz Högberg L., Heddini A, Cars O, The global need for effective antibiotics:
574 challenges and recent advances, Trends in Pharmacological Sciences, 2010, 31(11), 509–515.
575 DOI: 10.1016/j.tips.2010.08.002
576 [28] Becheker I, Berredjem H, Boutefnouchet N, Berredjem M, Ladjama A. Antibacterial
577 activity of four sulfonamide derivatives against multidrug-resistant Staphylococcus aureus.
578 Journal of Chemical and Pharmaceutical Research, 2014, 6, 893–899. DOI: 10.1186/1476-
579 0711-7-17
580 [29] Antonov L, Hansen PE, van der Zwan G. Comment on “Spectroscopic studies of keto–
581 enol tautomeric equilibrium of azo dyes” by M. A. Rauf, S. Hisaindee and N. Saleh, RSC
582 Adv., 2015, 5, 18097. RSC Advances, 2015, 5, 67165–67167. DOI: 10.1039/c5ra10553f
583 [30] Snavely FA, Yoder CH. A study of tautomerism in arylazopyrazolones and related
584 heterocycles with nuclear magnetic resonance spectroscopy. The Journal of Organic
585 Chemistry, 1968, 33, 513–515. DOI: 10.1021/jo01266a007
586 [31] Lestina GJ, Regan TH. The determination of the azo-hydrazone tautomerism of some 2-
587 pyrazolin-5-one dyes by means of nuclear magnetic resonance spectroscopy and 15N-labeled

588 compounds. The Journal of Organic Chemistry, 1969, 34, 1685–1686. DOI:
589 10.1021/jo01258a033
590 [32] Yoder CH, Barth RC, Richter WM, Snavely FA. A nuclear magnetic resonance study of
591 some nitrogen-15 substituted azo heterocycles. The Journal of Organic Chemistry, 1972,
592 37(25), 4121–4123. DOI: 10.1021/jo00798a034
593 [33] Rachedi Y, Hamdi M, Spéziale V. Synthesis of 4-Hydroxy-6-Methyl-3-β-Arylpropionyl
594 2-Pyrones by Selective Catalytic Hydrogenation of 3-Cinnamoyl-4-Hydroxy-6-Methyl 2-
595 Pyrones. Synthetic Communications, 1989, 19(20), 3437-3442. DOI:
596 10.1080/00397918908052752
597 [34] Rachedi Y, Hamdi M, Sakellariou M, Spéziale V. Reaction of 4-Hydroxy-6-Methyl-3-β-
598 arylpropionyl-2-Pyrones with Phenylhydrazine-Synthesis of a New Pyrazole Series. Synthetic
599 Communications, 1991, 20(10-11), 1189–1199. DOI: 10.1080/00397919108021038
600 [35] Wiley RH, Jarboe CH, 2-Pyrones. XVII. Aryl Hydrazones of Triacetic Lactone and Their
601 Rearrangement to 1-Aryl-3-carboxy-6-methyl-4-pyridazones. The Methyl Ether of Triacetic
602 Lactone, The Journal of the American Chemical Society, 1956, 78(3), 624–626. DOI:
603 10.1021/ja01584a028
604 [36] Matsuo K, Mori M, Syntheses of 10-Aryl-3-methyl-3,4-dihydro-1H-pyrano(4,3-
605 b)quinolin-1-ones, 3-Arylazo-4-hydroxy-6-methyl-5,6-dihydro-2H-pyran-2-ones, and 4-
606 Arylamino-3-(4-ethyl-1-piperazino)methyl-6-methyl-5,6-dihydro-2H-pyran-2-ones,
607 Chemistry Express, 1991, 6(7), 523–526. DOI: 10.1002/chin.199139154
608

Caption list of Figures, Tables and Schemes

Fig. 1. Synthetic strategy to azo dye structures **5** – **15**.

Fig.2 a. Absorption spectra of dye **5** (left) and **b.** dye **11** (right) in various solvents (black: n-hexane; red: dichloromethane; blue: acetone; violin: ethanol; green: acetonitrile).

Fig. 3. Absorption spectra of dyes **5** (blue) and **11** (red) in dichloromethane.

Fig. 4. UV-Vis absorption spectra of dyes **5** (violin), **6** (green), **7** (red), **8** (black) and **9** (blue) in ethanol.

Fig. 5. Molecular structures of monophenylhydrazones of 4-hydroxycoumarine **16** and *γ*-phenyl-*Δβ,γ*-butenolide **17**.

Fig. 6 a. Selected ^{1}H and ^{13}C NMR chemical shifts (right), **b.** HMBC correlations (left) of compound **10**.

Fig. 7 a. Selected ^{1}H and ^{13}C NMR chemical shifts (right), **b.** HMBC correlations (left) for compound **11**

Table 1 Influence of solvent on maximum wavelength of absorption (λ_{max}) of dyes **5** – **15**.

Table 2. Antibacterial screening data for inhibition zones of compounds **5** – **10** and new synthesized dyes **11** – **15** against different bacterial strains.

Table 3. Concentration and diameter of inhibition zone of compounds displaying the best antibacterial activity.

Table 4. *In vitro* antibacterial activity data in MIC (μg/ml) of tested compounds **5** – **10** and newly synthesized dyes **11** – **15** against different microbial species**.**

Table 5. Physical properties and yields of synthesized dyes

Scheme 1. Four possible tautomeric forms of the prepared azo dyes.

Scheme 2. Preparation of TAL **1** and DHTAL **2**.

Scheme 3. Preparation of diazonium salts **4a** – **f**.

Scheme 4. Synthetic route for the preparation of azo dyes **5 – 10**.

Scheme 5. Synthetic route for the preparation of azo dyes **11** – **15**.

638 **Graphical abstract**

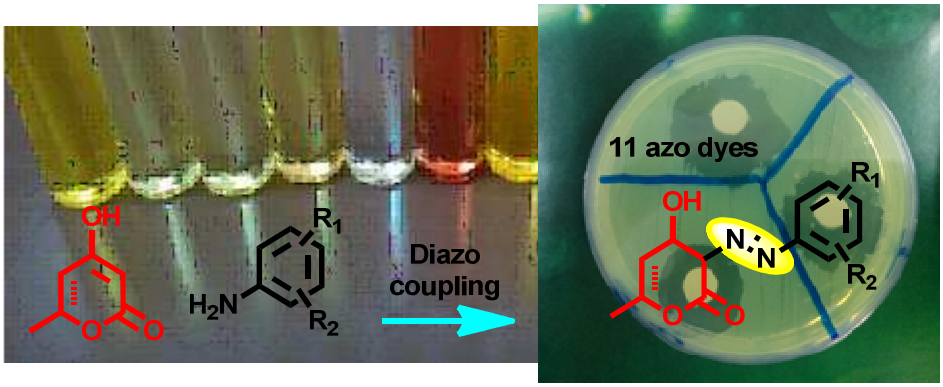

639

640